Appendix F

TIME-RESOLVED MOLECULAR CHARACTERIZATION OF ORGANIC AEROSOLS BY PILS + UPLC/ESI-Q-TOFMS

Zhang, X., N. Dalleska, D. Huang, K. Bates, A. Sorooshian, R. Flagan, and J. Seinfeld (2016). "Time-resolved molecular characterization of organic aerosols by PILS + UPLC/ESI-Q-TOFMS". In: *Atmos. Environ.* 130, pp. 180–189. DOI: http://doi.org/10.1016/j.atmosenv.2015.08.049.

Abstract

Real-time and quantitative measurement of particulate matter chemical composition represents one of the most challenging problems in the field of atmospheric chemistry. In the present study, we integrate the Particle-into-Liquid Sampler (PILS) with Ultra Performance Liquid Chromatography/Electrospray ionization Quadrupole Time-of-Flight High-Resolution/Mass Spectrometry (UPLC/ESI-Q-TOFMS) for the time-resolved molecular speciation of chamber-derived secondary organic aerosol (SOA). The unique aspect of the combination of these two well-proven techniques is to provide quantifiable molecular-level information of particle-phase organic compounds on timescales of minutes. We demonstrate that the application of the PILS + UPLC/ESI-Q-TOFMS method is not limited to water-soluble inorganic ions and organic carbon, but is extended to slightly water-soluble species through collection efficiency calibration together with sensitivity and linearity tests. By correlating the water solubility of individual species with their O:C ratio, a parameter that is available for aerosol ensembles as well, we define an average aerosol O:C ratio threshold of 0.3, above which the PILS overall particulate mass collection efficiency approaches ~0.7. The PILS + UPLC/ESI-Q-TOFMS method can be potentially applied to probe the formation and evolution mechanism of a variety of biogenic and anthropogenic SOA systems in laboratory chamber experiments. We illustrate the application of this method to the reactive uptake of isoprene epoxydiols (IEPOX) on hydrated and acidic ammonium sulfate aerosols.

F.1 Introduction

Chemical characterization of particulate organic compounds is crucial to understand the formation and evolution of secondary organic aerosol (SOA). The

conventional method for particle-phase molecular speciation is to collect aerosols on a filter substrate, followed by extraction and preconcentration. Analysis of filter extracts is commonly performed by liquid chromatography (LC) and gas chromatography (GC), coupled to mass spectrometry with the use of electron ionization (EI), chemical ionization (CI), electrospray ionization (ESI), and atmospheric pressure chemical ionization (APCI) (Dye and Yttri, 2005; Lavrich and Hays, 2007; Lin *et al.*, 2012; Simpson *et al.*, 2005; Surratt *et al.*, 2007a; Surratt *et al.*, 2007b; Surratt *et al.*, 2006; Szmigielski *et al.*, 2007). Major organic classes in SOA that have been identified from filter-based analysis include (nitrooxy)-organosulfates (Chan *et al.*, 2011; Iinuma *et al.*, 2007; Surratt *et al.*, 2007a; Surratt *et al.*, 2008, 2007b), dimers, trimers, and oligomers (Gao *et al.*, 2004; Jang *et al.*, 2002; Kalberer *et al.*, 2004; Limbeck *et al.*, 2003; Schilling Fahnestock *et al.*, 2015), and humic-like substances (Gelencser *et al.*, 2002; Graham *et al.*, 2002). A limitation of filter-based analysis is low time resolution and, consequently, the inability to track particle-phase kinetics. In addition, filter artifacts, such as adsorption of ambient vapors and evaporation of semi-volatile compounds from the filter surface, lead to uncertainties in the quantification of particle-phase components (Dzepina *et al.*, 2007; Schauer *et al.*, 2003; Turpin *et al.*, 2000).

Powerful, on-line techniques have been developed for chemical speciation of organic aerosols, with rapid time response and minimum sample handling. The general principle is to vaporize airborne aerosols by thermal or laser desorption, followed by ionization and mass spectrometric detection (Canagaratna *et al.*, 2007; Sullivan and Prather, 2005). The Aerodyne Aerosol Mass Spectrometer (AMS), which is now a routine component of ambient and chamber studies, enables measurement of organic fragments and derivation of the atomic O:C and H:C ratios (Aiken *et al.*, 2007; Aiken *et al.*, 2008; Jimenez *et al.*, 2003). Identification of individual species by AMS is not available due to the high evaporation temperature (600 °C) and EI energy (70 eV), which result in significant molecular fragmentation. Moreover, all thermal/laser desorption methods are susceptible to fragmentation of non-refractory compounds. To achieve unambiguous molecular identification of particulate organic compounds, extensive fragmentation is avoided by employing soft ionization techniques such as chemical ionization (Aljawhary *et al.*, 2013; Hearn and Smith, 2004; Hellen *et al.*, 2008; Hoffmann *et al.*, 1998; Lopez-Hilfiker *et al.*, 2014; Smith *et al.*, 2005; Yatavelli and Thornton, 2010), photoelectron resonance capture ionization (LaFranchi and Petrucci, 2006; Zahardis *et al.*, 2006), and vacuum ultraviolet single photon ionization (Ferge *et al.*, 2005; Isaacman *et al.*, 2012; Northway *et al.*, 2007;

Oktem *et al.*, 2004). Full-scale implementation of these methods into routine measurements requires achieving short measurement cycles, resolving quantification capability, interpreting the mass spectral complexity, and comparing data recovery with conventional methods.

The Particle-into-Liquid Sampler (PILS), first developed by Weber *et al.* (2001), grows aerosols by supersaturated water vapor condensation, producing droplets sufficiently large for collection by inertial impaction. The resulting liquid samples can be analyzed by ion chromatography (IC) for water-soluble inorganic ions and small dicarboxylic acids (Ma *et al.*, 2004; Oakes *et al.*, 2010; Orsini *et al.*, 2003; Rastogi *et al.*, 2009; Sorooshian *et al.*, 2008; Sorooshian *et al.*, 2007), or by a total organic carbon analyzer (TOC) for the total water soluble organic carbon (WSOC) (Peltier *et al.*, 2007; Sullivan *et al.*, 2006). PILS coupled with mass spectrometry has also been deployed for the analysis of WSOC in field and chamber measurements. Bateman *et al.* (2010) compared the off-line mass spectra of limonene + O_3 derived SOA samples collected by PILS with those collected on filter substrates and found that the peak abundance, organic mass to organic carbon ratios, and the average O:C ratio are essentially identical. Parshintsev *et al.* (2010) integrated PILS on-line with a solid-phase extraction chromatographic system for the characterization of organic acids. Using a similar concept, Clark *et al.* (2013) directly injected PILS samples into the ionization source of the mass spectrometer and validated the PILS-ToF-MS system against other particle measurement methods in terms of total ion abundance and average O:C ratios of isoprene and α-pinene derived SOA.

A primary challenge in the deployment of PILS as an effective particle collection device lies in the determination of the overall mass collection efficiency. Ambient and chamber derived organic aerosols usually comprise of thousands of species with various physicochemical properties. Since PILS was originally designed to use water steam as the growing agent, one expects that particles with an extreme hydrophobic surface would be difficult to collect. Therefore, a guideline needs to be developed for the reference of PILS selectivity to certain types of aerosols. This is one main focus of the present study.

Here we combine PILS with Ultra Performance Liquid Chromatography/ Electrospray Ionization Quadrupole Time-of-Flight High-Resolution Mass Spectrometry (UPLC/ESI-Q-TOFMS), for time-revolved molecular-level characterization of SOA during chamber experiments. This technique is particularly suited to polar or water-soluble organic molecules, and potentially high molecular weight species, such

as organosulfates. Advantages of this technique include: 1) No need for sample preparation; 2) Molecular-level information can be inferred from the electrospray ionization process, in which ions are, in general, observed as those of the parent molecule with the addition of an H atom (positive mode) or removal of an H atom (negative mode); 3) Temporal profiles of particle composition can be obtained on a time scale consistent with that of SOA evolution; and 4) Chromatographic separation of organic compounds with different polarities avoids the analyte signal suppression that occurs during the electrospray process of organic mixtures, leading to molecular-level quantification of particle-phase constituents. We demonstrate that the PILS + UPLC/ESI-Q-TOFMS method is suitable to measure water-soluble organic carbon (WSOC), as well as less hydrophilic or slightly water-soluble compounds. A collection efficiency of >0.6 can be achieved for chamber-derived SOA systems with average O:C ratios >0.3. We illustrate the application of this technique to the reactive uptake of isoprene epoxydiols (IEPOX) on hydrated and acidic ammonium sulfate aerosols.

F.2 Experimental Methods

F.2.1 Pure Component Organic Aerosols

Table F.1 gives the chemical properties of organic standards (purchased from Sigma Aldrich) that were used to generate pure component organic aerosols. These standards include carboxylic acids, amines, and polyols that span a broad range in water solubility from miscible to insoluble, and vapor pressure from intermediate to low volatility. Each standard was dissolved in water or isopropanol to produce a concentrated solution. Aerosols with known chemical composition were produced by atomizing each single concentrated solution followed by desolvation. Two diffusion denuders filled with silica gel and activated carbon were used to remove the solvent prior to injection into the Caltech 24 m^3 Teflon chamber. Relative humidity (RH) and temperature in the chamber were maintained at <5% and 25 °C, respectively. The size distribution and number concentration of the pure component organic aerosols were measured continuously using a custom-built scanning mobility particle sizer (SMPS) consisting of a differential mobility analyzer (DMA, TSI, 3081) coupled with a condensation particle counter (CPC, TSI, 3010). More details of the SMPS operation can be found in Loza *et al.* (2014), Zhang *et al.* (2014a), and Zhang *et al.* (2014b).

compound	chemical formula	exact mass	*m/z* (error/mDa)	water solubility at 20 °C	vapor pressure (atm at 298 K)
Adenine	$C_5H_5N_5$	135.0545	$[M+H]^+$ (1.6)	0.103 g L^{-1}	8.117×10^{-5}
Adonitol	$C_5H_{12}O_5$	152.0685	$[M-H]^-$ (4.8)	50.0 g L^{-1}	7.711×10^{-12}
Adipic acid	$C_6H_{10}O_4$	146.0579	$[M-H]^-$ (0.6)	0.25 g L^{-1}	3.292×10^{-9}
d-Sorbitol	$C_6H_{14}O_6$	180.0634	$[M-H]^-$ (2.5)	182.0 g L^{-1}	2.424×10^{-14}
Diethylmalonic acid	$C_7H_{12}O_4$	160.0736	$[M-CO_2-H]^-$ (0.1)	25.0 g L^{-1}	2.696×10^{-9}
Vanillic acid	$C_8H_8O_4$	168.0423	$[M-H]^-$ (-1.8)	1.5 g L^{-1}	7.940×10^{-10}
Azelaic acid	$C_9H_{16}O_4$	188.1049	$[M-H]^-$ (-4.2)	2.14 g L^{-1}	1.151×10^{-10}
cis-Pinonic acid	$C_{10}H_{16}O_3$	184.1099	$[M-H]^-$ (1.9)	7.8 g L^{-1}	1.485×10^{-7}
Myristic acid	$C_{14}H_{28}O_2$	228.2089	$[M-H]^-$ (0.7)	20.0 mg L^{-1}	6.711×10^{-9}
Palmitic acid	$C_{16}H_{32}O_2$	256.2402	$[M-H]^-$ (1.3)	7.2 mg L^{-1}	7.175×10^{-10}

Table F.1: Compounds used for method development. Water solubility data are from Yaws (2003), and vapor pressure is estimated by taking the average of predictions from the 'Evaporation' (Compernolle *et al.*, 2011) and 'SIMPOL.1' (Pankow and Asher, 2008) models.

F.2.2 Particle-into-Liquid Sampler (PILS)

Detailed characterization of the Caltech PILS, which is based on a modification of the original design of Weber *et al.* (2001), is described by Sorooshian *et al.* (2006). The chamber aerosol is sampled through a 1 μm cut size impactor with a flow rate of 12.5 L min^{-1}, and passed successively through individual acid and base gas denuders and an organic carbon denuder to remove inorganic and organic vapors. A steam flow generated at 100 °C is adiabatically mixed with the cooler sampled air in a condensation chamber, creating a high water supersaturation environment in which particles grow sufficiently large (D_p > 1 μm) for collection by inertial impaction onto a quartz plate. Impacted particles are transported to a debubbler by a washing flow (0.15 mL min^{-1}) comprising 50% water and 50% isopropanol. The sampled liquid is delivered into vials held on a rotating carousel. This design is especially beneficial for the application of liquid chromatography for organic compound separation and selection, which generally requires a longer time than the PILS collection cycle. Under the current configuration, a 5 min time resolution can be achieved for the characterization of particle-phase dynamics.

F.2.3 UPLC/ESI-Q-TOFMS

The PILS collected samples are stored at 4 °C and analyzed by UPLC/ESI-Q-TOFMS within 24 h without further pretreatment. A WATERS ACQUITY UPLC I-Class System, coupled with a Quadrupole Time-of-flight Mass Spectrometer (Xevo G2-S QToF) and equipped with an electrospray ionization (ESI) source, was used to identify and quantify the PILS collected samples, including organic aerosol

standards and chamber generated SOA. An ACUITY BEH C_{18} column (2.1 × 50 mm) was used to separate relatively nonpolar species, including vanillic acid, azelaic acid, *cis*-pinonic acid, myristic acid, palmitic acid, and IEPOX-derived SOA. The eluent program is: 0-3.2 min: 100% A (0.1% formic acid in water); 3.2-3.5 min: 10% A and 90% B (acetonitrile); 3.5-5 min: 100% A. The total flow rate is 0.5 mL min^{-1} and the injection volume is 5 μL. For extremely polar or water soluble compounds, including adenine, adonitol, adipic acid, d-sorbitol and diethylmalonic acid, an ACUITY BEH Amide column (2.1 × 150 mm) was used for species separation. The eluent program is: 0-3 min: 5% A (10 mM ammonium formate in water at pH = 9) and 95% B (acetonitrile); 3-3.01 min: 45% A and 55% B; 3.01-8 min: 5% A and 95% B. The total flow rate is 0.6 mL min^{-1} and the injection volume is 4 μL. Note that the eluent program used here is customized for the characterization of test aerosols that are composed of a single chemical standard. For chamber-derived SOA samples that might contain thousands of species with a variety of polarities, key parameters of the eluent program, such as the type and ratio of polar vs. nonpolar solvents, the additives and pH range in the mobile phase, and the overall elution duration, need to be optimized to achieve compound specificity. The choice of separation modes is also very important. For extremely polar compounds, hydrophilic-interaction chromatography is a more suitable approach, compared with reverse-phase chromatography, which has been, though, widely used in particle-phase speciation in previous studies. Optimum electrospray conditions are: 2.0 kV capillary voltage, 40 V sampling cone, 30 V source offset, 120 °C source temperature, 350 °C desolvation temperature, 30 L h^{-1} cone gas, and 650 L h^{-1} desolvation gas. MS/MS spectra were obtained by applying a collision energy ramping program starting from 15 eV to 50 eV over one MS scan in the collision cell. Accurate masses were corrected by a lock spray of leucine encephalin (*m/z* 556.2771 $[M+H]^+$). Data were acquired and processed using the MassLynx v4.1 software.

F.3 Method evaluation

F.3.1 Simulation of Hygroscopic Growth of Organic Aerosols

The operational principle of the PILS is to grow particles in the presence of supersaturated water vapor to the size of micro-droplets that can be collected by inertial impaction. A key parameter that governs the extent of particle growth is the water accommodation coefficient (α_w), which is defined as the fraction of water molecules that are taken up by the particles upon collision with the surface. Here we

investigate numerically the influence of α_w on the predicted final size of the droplets by condensational growth of particles.

The growth of a particle of diameter D_p in the presence of supersaturated water vapor is governed by (Seinfeld and Pandis, 2006):

$$\frac{dD_p}{dt} = \frac{4 \cdot D_w \cdot M_w}{R \cdot T \cdot D_p \cdot \rho_p} \left[p_w^{\infty} - p_w^s(D_p, T_s) \right] \cdot f(Kn, \alpha_w) \tag{F.1}$$

where D_w is the water vapor diffusivity, M_w is the water molecular weight, R is the gas constant, T is the temperature, ρ_p is the particle density, Kn (=$2\lambda/D_p$) is the Knudsen number, $f(Kn, \alpha_w)$ is the correction factor for noncontinuum conditions and imperfect accommodation, p_w^{∞} is the water saturation vapor pressure far from the particle, and $p_w^s(D_p, T_s)$ is the water vapor pressure over the particle surface. Taking into account the vapor pressure variation due to the Kelvin effect, $p_w^s(D_p, T_s)$ becomes:

$$p_w^s(D_p, T_s) = p_w^0(T_s) \cdot \chi_w \cdot \gamma_w \cdot exp\left(\frac{4 \cdot \sigma \cdot \nu_l}{R \cdot T \cdot D_p} \right) \tag{F.2}$$

where $p_w^0(T_s)$ is the water saturation vapor pressure at the particle temperature T_s, χ_w is the mole fraction of water in the particle phase, σ is the water surface tension, ν_l is the water molar volume, and γ_w is the water activity coefficient, which is assumed to be unity here. Note that particles in the PILS condensation chamber are assumed to behave as a dilute solution so that γ_w approaches its infinite dilution limit $\gamma_w \rightarrow 1$. This is reasonable considering that the water volume fraction exceeds 0.93 in particles after 0.1 s of hygroscopic growth. The water activity coefficient deviates from unity (<1) in non-ideal organic-salt-water mixtures (Zuend *et al.*, 2008, 2010), which is the case during the initial particle growth stage in the PILS condensation chamber. This leads to an overestimate of the water vapor partial pressure over the particle surface, and consequently, slower simulated particle growth rate due to water condensation. In other words, the actual particle hydroscopic growth rate in the PILS condensation chamber should be faster than the model simulations.

The particle surface temperature is determined by an energy balance on the particle (Seinfeld and Pandis, 2006):

$$\Delta T = \frac{\Delta H_v \cdot D_w \cdot \rho_w}{k_a' \cdot T_{\infty}} \cdot \left[S_{w,\infty} - exp\left(\frac{\Delta H_v \cdot M_w}{R \cdot T_{\infty}} \cdot \frac{\Delta T}{1 + \Delta T} + \frac{4 \cdot \sigma \cdot \nu_l}{R \cdot T \cdot D_p} \right) \right] \cdot f(Kn, \alpha) \tag{F.3}$$

where $\Delta T = (T_s - T_{\infty})/T_{\infty}$, ΔH_v is the latent heat of vaporization of water, ρ_w is the density of water steam, k_a' is the effective thermal conductivity of air corrected

for noncontinuum effects, and $S_{w,\infty} = p_w^{\infty}/p_w^0(T_\infty)$ is the environmental saturation ratio. Equation F.3 needs to be solved numerically to determine the particle surface temperature that is required in the calculation of the particle growth rate.

Figure F.1 shows the predicted hygroscopic growth of particles, with initial diameters ranging from 20 nm to 800 nm, as a function of water accommodation coefficient (α_w). Particles with highly hydrophilic surface composition ($\alpha_w \rightarrow 1$) can grow sufficiently large ($D_p > 1$ μm) to be collected by inertial impaction within 1 s, the particle residence time in the PILS condensation chamber. Water vapor mass transfer to less hydrophilic particles ($\alpha_w \leq 10^{-2}$) is still sufficiently rapid to grow particles to droplets >1 μm size. Significant kinetic reductions in water uptake result when the particle-phase constituents are strongly hydrophobic ($\alpha_w \leq 10^{-3}$). The effect of initial relative humidity (RH) in aerosol sampling flow on the ultimate droplet size becomes critical when α_w is $\sim 10^{-3}$. The simulations suggest that PILS can potentially collect particles with a wide range of water solubility, due to the substantial imbalance in water vapor abundance far from and over the particle surface. As discussed earlier, the assumption of ideal water-ion-organic interactions leads to the underestimation of particle hygroscopic growth rate. As a result, the specification of α_w in the order of $\sim 10^{-3}$ as a criterion for "hydrophobic" particles that fail to grow over 1 μm diameter might be a bit conservative.

F.3.2 Collection Efficiency

The PILS collection efficiency may deviate from unity owing to three processes: 1) particle losses due to gravitational settling, diffusion, and inertial deposition during transport in the PILS plumbing system and condensation chamber, 2) evaporation of semi-volatile components during adiabatic mixing with steam, and 3) imperfect accommodation of water vapor on particles, if hydrophobic (Orsini *et al.*, 2003; Sorooshian *et al.*, 2006; Weber *et al.*, 2001). In the present study, we characterize the PILS collection efficiency by varying the particle chemical composition (*i.e.*, polarity and volatility) and size distribution. The overall mass collection efficiency (CE_{PILS}) can be obtained by comparing the mass concentration measured by the UPLC/ESI-Q-TOFMS and that derived from the DMA measured particle volume distribution, assuming particle sphericity (Sorooshian *et al.*, 2006):

$$CE_{PILS} = \frac{1000 \cdot m \cdot Q_l \cdot DF \cdot \rho_l}{Q_g \cdot \rho_p \cdot V_p} \tag{F.4}$$

where 1000 is the unit conversion factor, m is the UPLC/ESI-Q-TOFMS measured organic standard mixing ratio (ppm), Q_l is the liquid sampling flow rate (1.5 mL

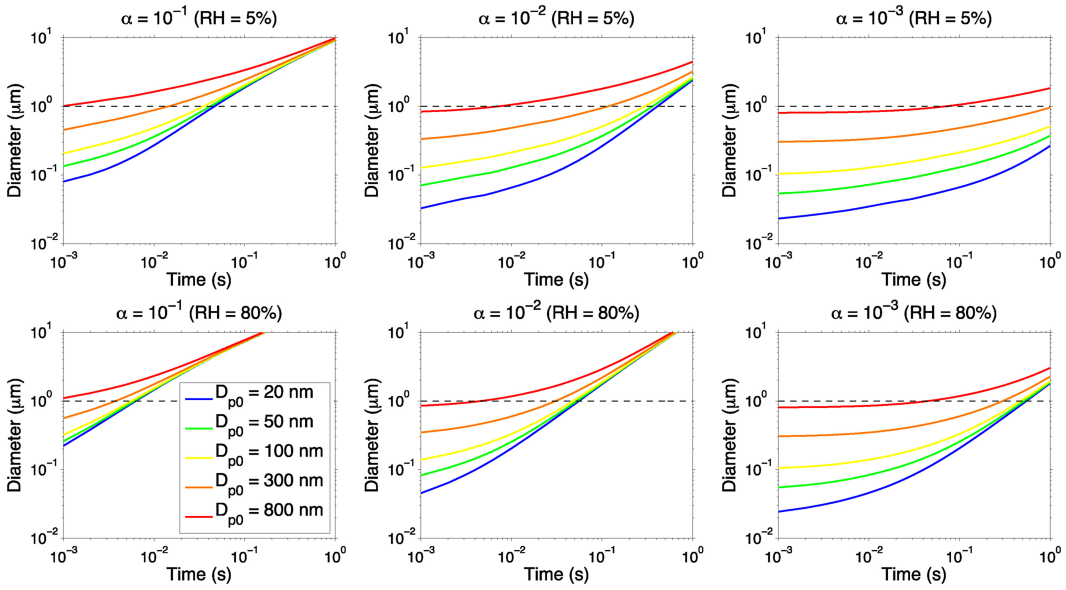

Figure F.1: Simulations of particle condensational growth over an initial size range of 20-800 nm diameter in the presence of supersaturated water vapor for different assumed water accommodation coefficients (α_w = 10^{-3}, 10^{-2}, and 10^{-1}) at initial relative humidities (RH) of 5% (upper panel) and 80% (lower panel) in the chamber. The black dashed line denotes the threshold value (1 μm in diameter) of particle size for effective PILS collection.

min^{-1}), DF is the dilution factor that accounts for the water vapor condensation on the impactor wall and air bubbles during the filling of vials, ρ_l is the density of collected liquid, which is assumed as the density of the washing flow (0.893 g cm^{-3}), Q_g is the gas sampling flow rate (12.5 L min^{-1}), V_p is the particle total volume concentration (μm^3 cm-3) derived from the DMA measured number distribution, and ρ_p is the particle density (g cm^{-3}). Note that ρ_p here is assumed as the density of corresponding chemical standards that are used to generate test aerosols. For chamber-derived SOA, ρ_p can be derived from the AMS measured O:C and H:C ratios (Kuwata *et al.*, 2012). A 5 min offset in the PILS measurement is taken into account to retrieve the particle concentration at the moment of entry into the PILS inlet.

Figure F.2 shows the measured PILS mass collection efficiency (CE_{PILS}) as a function of particle water solubility and volatility. Consistent with the model prediction, the high collection efficiency in the PILS is achieved not only for highly water soluble and non-volatile aerosols such as sorbitol, but also for slightly water soluble and intermediate/semi-volatile aerosols such as pinonic acid. The water solubility of particle-phase constituents clearly governs CE_{PILS}. The effect of

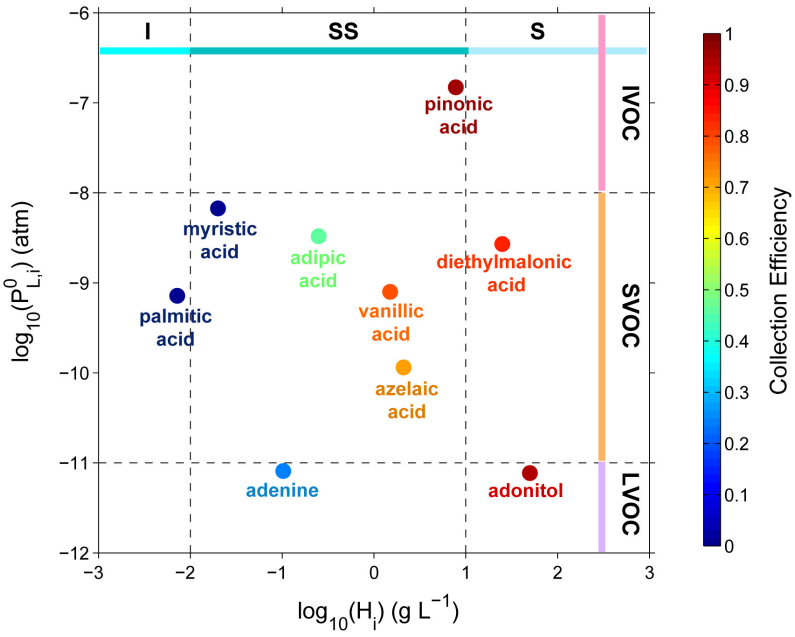

Figure F.2: Measured PILS overall mass collection efficiency for the test organic aerosols as a function of volatility, which is defined as the vapor pressure of compound i as pure liquid at 20 °C on the logarithm scale ($\log_{10}P^0_{L,i}$, atm), and water solubility, which is defined here as the maximum amount of the compound i that will dissolve in pure water at 20 °C on the logarithm scale ($\log_{10}H_i$, g L^{-1}). Compound volatility is categorized according to intermediate volatility organic compound (IVOC), semi-volatile organic compound (SVOC), and low volatility organic compound (LVOC). Water solubility is categorized broadly as insoluble (I), slightly soluble (SS), and soluble (S).

volatility on CE_{PILS}, however, is not discernable, indicating that the evaporation of semi-volatiles from particles during adiabatic mixing with steam is negligible for compounds with vapor pressure $<10^{-6}$ atm. We define the particle water solubility threshold of 1 g L^{-1} above which >0.6 mass collection efficiency can be achieved. Considering that SOA water solubility data are generally unavailable, this quantity can be related to the average particle O:C ratio, which is relatively well constrained by the AMS measurement.

Figure F.3 shows the water solubilities (the maximum amount of the compound i that will dissolve in pure water at 20 °C on the logarithm scale, $\log_{10}H_i$/g L^{-1}) of a variety of organic compounds, including carboxylic acids, alcohols, carbonyls, esters, and ethers, as a function of their O:C ratios. Regardless of the nature of functionalities in the molecule, the water solubility increases with the O:C ratio and eventually reaches a plateau, a miscible state with water. The O:C ratio correspond-

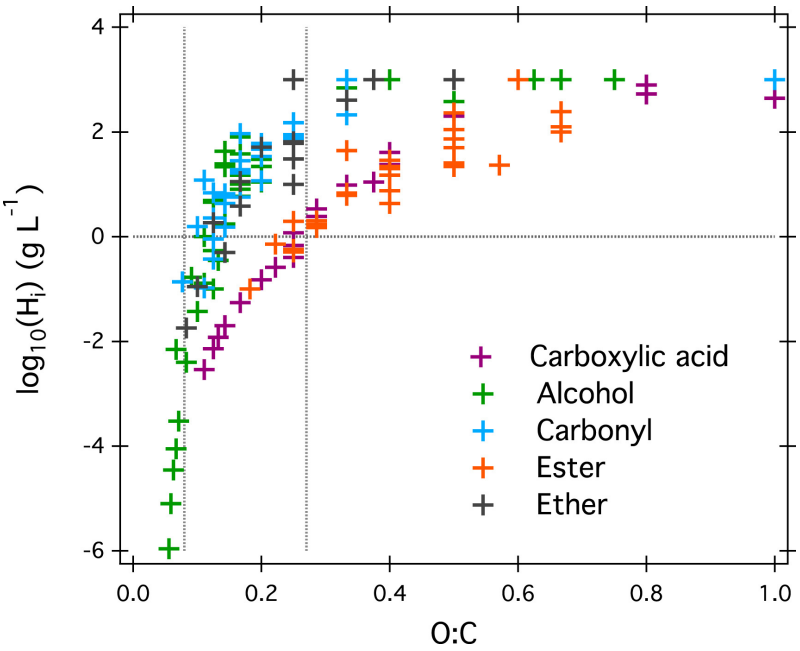

Figure F.3: Water solubility of carboxylic acid, alcohol, carbonyl, ester, and ether standards at 20 °C as a function of their O:C ratios. Each data point represents an individual compound with certain functionalities. The horizontal gray line represents the water solubility threshold (1 g L^{-1}) at which the PILS collection efficiency of ~0.6 will be achieved. The two vertical gray lines define a region of average particle O:C ratios that correspond to the water solubility threshold. Data source: Yaws (2003).

ing to the water solubility threshold of 1 g L^{-1} varies with functionalities, ranging from 0.07 to 0.26. Considering that SOA is generally a mixture of species that might contain all the functional groups above, we suggest that the upper limit of the O:C ratio, 0.26, represents a criterion to constrain an effective PILS mass collection efficiency. The AMS measured O:C ratios for SOA produced from isoprene + OH, α-pinene + O_3/OH, aromatics + OH, and C_{12}-alkane + OH in the Caltech Environmental Chamber have been summarized previously (Chhabra *et al.*, 2010, 2011; Loza *et al.*, 2014; Zhang and Seinfeld, 2013). Among all the systems investigated, long-chain alkane derived SOA exhibits the lowest O:C ratio, ranging from ~0.2 to ~0.3, over the course of 3-36 h experiments ([OH] exposure = 2-8 molecules cm^{-3} h). The average O:C ratios measured from other SOA systems, on the other hand, exceed the threshold, 0.26, at which >0.6 mass collection efficiency by PILS can be achieved. Thus, PILS is a candidate as a high efficiency, time-resolved particle collection method for a majority of SOA systems.

Particles are subject to gravitational settling, diffusion, and inertial deposition in

the PILS plumbing system and condensation chamber. The largest losses occur for small (D_p < 10 nm) and large particles (D_p > 1000 nm), as predicted to be 2.2% and 8.6%, respectively (Sorooshian *et al.*, 2006). Considering that the PILS transmission efficiency (defined as the fraction of particles of a certain size that are transported through the PILS plumbing system and condensation chamber) depends strongly on the particle size, the impact of variations in the particle size distribution on the PILS overall mass collection efficiency (CEPILS) is at issue. For a typical SOA chamber experiment, the initial size distribution of seed particles spans from ~20 nm to ~600 nm, with a median diameter of ~60-70 nm. Growth driven by gas-phase photochemistry and gas-particle partitioning occurs primarily on large particles and, as a result, the number median diameter shifts to ~200 nm after ~20 h of irradiation. To mimic the progression of the particle size distribution during SOA formation, test particles were initially generated by atomizing concentrated pinonic acid solution into the chamber. An external flow pulse creates intense turbulent mixing in the chamber. As a result, the median diameter of the *cis*-pinonic acid particles shifted from ~90 nm to ~200 nm during the 3.5 h experiment, due to rapid deposition of the smaller particles onto the chamber wall (see Figure F.4). The overall PILS mass collection efficiency, on the other hand, remains consistently close to unity, within ~8% uncertainty. This test demonstrates that change in particle size distribution during SOA formation and evolution under typical chamber experimental conditions does not significantly impact the PILS collection efficiency.

F.3.3 Sensitivity, Detection Limit, and Uncertainties

The extent of linearity of UPLC/ESI-Q-TOFMS detected signals for PILS collected organic aerosols was examined in response to changes in particle mass loadings. Sorbitol, azelaic acid, pinonic acid, and adipic acid aerosols, with mass concentrations ranging from 20 to 300 μg m^{-3}, were generated by varying the atomization and dilution duration. Mass concentrations of these four organic aerosol standards were derived from the SMPS measured particle volume distribution. The UPLC/ESI-Q-TOFMS signals for sorbitol, azelaic acid, and pinonic acid, as shown in Figure F.5, exhibit linearity (R^2 = 0.99) with organic mass loadings. The sensitivity for adipic acid, however, is drifting low when particle concentrations are diluted, and as a result, there is a strong negative offset in the linear fitting curve. The low sensitivity for adipic acid might be attributed to the slight solubility of adipic acid dimer, which is the dominant particle-phase form of adipic acid (Wolfs and Desseyn, 1996).

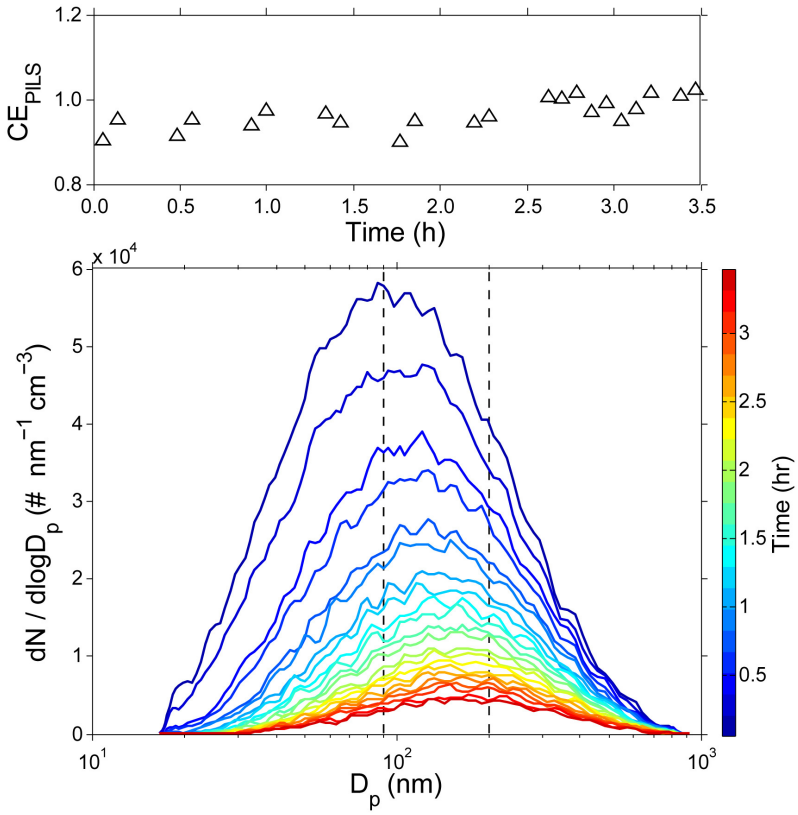

Figure F.4: PILS overall mass collection efficiency (upper panel) for *cis*-pinonic acid aerosols as a function of particle number distribution (lower panel). Over ~3 h, aerosol wall deposition from intense turbulent mixing in the chamber caused the number median aerosol diameter to shift from 90 nm to 200 nm.

The detection limit of the PILS + UPLC/ESI-Q-TOFMS system can be estimated from the expected UPLC/ESI-Q-TOFMS sensitivity and measured flow rates of sampling air and liquid washing stream. The UPLC/ESI-Q-TOFMS detection limit (LOD) was calculated according to the expression:

$$\frac{S}{N} = \frac{k_i \cdot LOD}{\sigma} \tag{F.5}$$

where S/N is the signal-to-noise ratio, k_i is the response factor or the sensitivity of UPLC/ESI-Q-TOFMS for species i, and σ is the standard deviation of the response. Using a signal-to-noise ratio of 2, LOD of 0.68 ppb is obtained for *cis*-pinonic acid as an example. With a gas flow rate of 12.5 L min^{-1}, and a washing flow rate of 0.15 mL min^{-1}, the PILS + UPLC/ESI-Q-TOFMS system is estimated to have a detection limit of 19.02 ng m^{-3} for *cis*-pinonic acid in the particle phase. By analogy with other compounds that are selected by UPLC, the sensitivity of the Q-TOFMS technology can be practically achieved as low as ~ ppb level. Thus

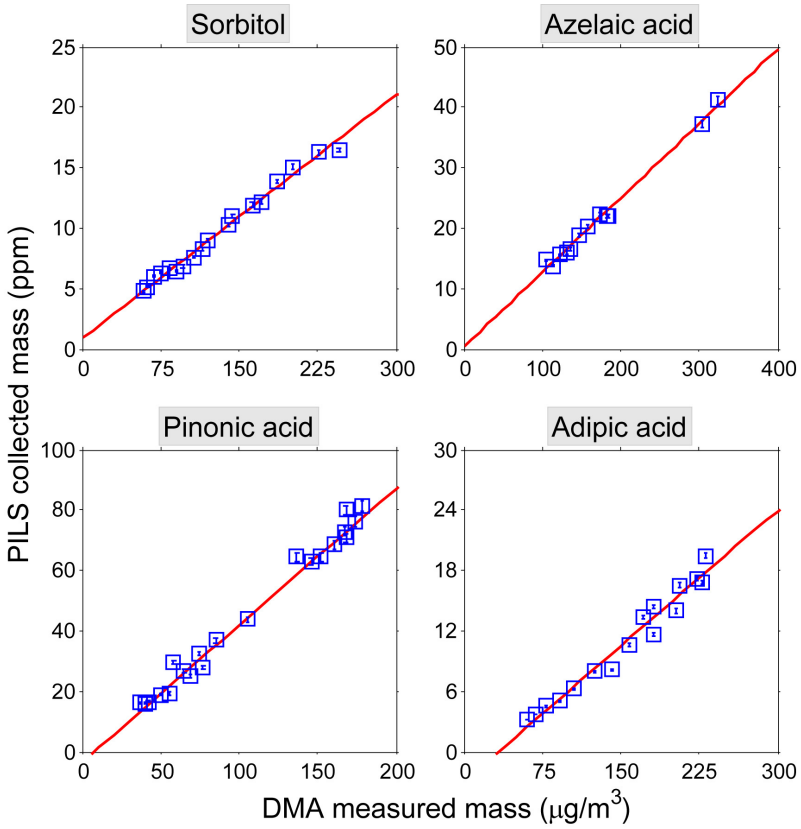

Figure F.5: UPLC/ESI-Q-TOFMS measured mass concentration of sorbitol, azelaic acid, pinonic acid, and adipic acid in PILS samples versus the DMA-measured total particle mass. Linear fits to the data are shown with the mean R^2 = 0.99.

we expect the detection limit of PILS + UPLC/ESI-Q-TOFMS measurement of the mass of particle components in the range of tens of ng m^{-3} to a few μg m^{-3}.

Uncertainties in the PILS + UPLC/ESI-Q-TOFMS measurement arise mainly from variation of the collected liquid volume due to the existence of air bubbles. Specifically, the washing flow carries the impacted droplets *via* a stainless steel mesh wick on the perimeter of the impactor to a 'T-shape' debubbler. Air bubbles are vacuumed out of the system by a peristaltic pump. The liquids are delivered into the injection needle that is inserted into individual vials by two syringe pumps. Perfect debubbling cannot always be achieved and as a result, the collected liquid volumes in some vials can drift low. The measurement uncertainties due to the existence of air bubbles in the liquid samples are estimated to be <11% by weighing a batch of vials over one carousel running cycle (72 vials). Repeatability in the detected yield of ions from the electrospray ionization of the analyte is another potential origin of measurement uncertainties. This was estimated to be <3% by

repeating injection of 4 μL standard organic samples into the electrospray source. The effect of ESI-MS sensitivity drift on the measurement accuracy is accounted for by regularly performing the repeatability of organic standards (one standard every ten samples) during routine sample analysis.

While the PILS + UPLC/ESI-Q-TOFMS system is demonstrated to achieve time-resolved molecular speciation of secondary organic aerosols, we acknowledge the potential artifacts and uncertainties arising from aerosol sampling and analysis procedures. First, the hydrolysis of labile functionalities, mainly including organic nitrates, carbonyls, and epoxides, upon solvation is inevitable in any aerosol collection, pretreatment and analysis procedures using water as the solvent. Second, water steam (100 ± 2 °C) is mixed with aerosol sample flow (25 ± 5 °C) in the PILS condensation chamber, with temperature eventually stabilized as ~36 °C. During mixing, organic aerosol constituents are subjected to evaporation and thermal decomposition. We have demonstrated earlier that the evaporation of semivolatile organic compounds is not significant during adiabatic mixing (Figure F.2). Steady decomposition of thermally labile compounds in neutral solution, such as organic peroxides, requires a temperature higher than ~80 °C (Hart, 1949). Considering that the residence time of the PILS condensation chamber is only 1 s, it is expected that the original structure of thermally labile organic molecules should be mostly intact in such a short timescale.

F.4 Method Application: IEPOX Uptake onto Acidified and Hydrated Ammonium Sulfate Particles

The heterogeneous chemistry of isoprene epoxydiols (IEPOX), a second generation product formed from isoprene photochemistry in the absence of NO, contributes significantly to the SOA formation (Lin *et al.*, 2014, 2012; Nguyen *et al.*, 2014a; Paulot *et al.*, 2009b; Surratt *et al.*, 2010). Proposed mechanisms leading to SOA production involve the ring opening of the epoxide group, followed by the addition of available nucleophiles in the condensed phase, *e.g.*, tetrol production *via* the addition of water and organosulfate production *via* the addition of sulfate (Eddingsaas *et al.*, 2010; Nguyen *et al.*, 2014a; Surratt *et al.*, 2010). The PILS + UPLC/ESI-Q-TOFMS method was employed to characterize the SOA formation and evolution *via* the reactive uptake of IEPOX onto hydrated and acidified ammonium sulfate particles. The IEPOX-derived SOA is a well-established system to test the performance of the PILS + UPLC/ESI-Q-TOFMS technique.

F.4.1 Chamber experiment and instrument operation protocols

The experiment was conducted in the Caltech 24 m^3 Environmental Chamber maintained at 20 °C. Detailed experimental protocols are presented in an earlier study (Nguyen *et al.*, 2014a). The general experimental procedure is as follows: 1) flushing the chamber with purified dry air for 24 h prior to the experiment; 2) humidifying the chamber to ~78% RH by passing purified air through a Nafion membrane humidifier (FC200, Permapure LLC) that is kept wet by recirculation of 27 °C ultra-pure water (18 MΩ, Millipore Milli-Q); 3) Injecting inorganic seed aerosols by atomizing an acidified ammonium sulfate aqueous solution (0.06 M $(NH_4)_2SO_4$ + 0.06 M H_2SO_4) followed by a custom-built wet-wall denuder; and 4) injecting the gas-phase trans β-IEPOX isomer by evaporating several droplets in a glass bulb with 6 L min^{-1} of purified and heated dry air (60 °C) for ~ 100 min.

The gas-phase IEPOX mixing ratio was monitored using a custom-modified Varian 1200 triple-quadrupole chemical ionization mass spectrometer (CIMS). In negative mode operation, CF_3O^- was used as the reagent ion to cluster with the analyte [R], producing $[R{\cdot}CF_3O]^-$ or *m/z* $[M+85]^-$, where M is the molecular weight of the analyte. More details on the CIMS operation and data analysis are given by Zhang *et al.* (2015). Real-time particle mass spectra were collected continuously by an Aerodyne High Resolution Time-of-Flight Aerosol Mass Spectrometer (HR-AMS). The AMS switched once every minute between the high resolution 'W-mode' and the lower resolution, higher sensitivity 'V-mode'. The V-mode was utilized for quantification, as the higher *m/z* values exhibit a more favorable signal-to-noise ratio. The W-mode was used for ion identification and clarification. More details on AMS operation and data analysis are given by Nguyen *et al.* (2014a).

F.4.2 Results and Discussions

Shown in Figure F.6 (upper panel) are the CIMS signals at *m/z* (-) 203, which represents the fluoride cluster product of IEPOX ($C_5H_{10}O_3{\cdot}CF_3O^-$), and organic particulate mass concentrations measured by the HR-AMS. Dominant ions observed in the HR-AMS spectra include *m/z* 29, *m/z* 43, *m/z* 53 (mostly $C_4H_5^+$) and *m/z* 82 (mostly $C_5H_6O^+$). The latter two are considered as the tracers for IEPOX derived organic aerosols (Budisulistiorini *et al.*, 2013; Lin *et al.*, 2012). The time-dependent trend of gas-phase IEPOX measured by CIMS during the injection period (0-100 min) is almost identical to the AMS measured total particulate organics, indicating the uptake of IEPOX and the subsequent reactions are essentially instantaneous. Gas-particle equilibrium is rapidly established after the IEPOX injection. Over the

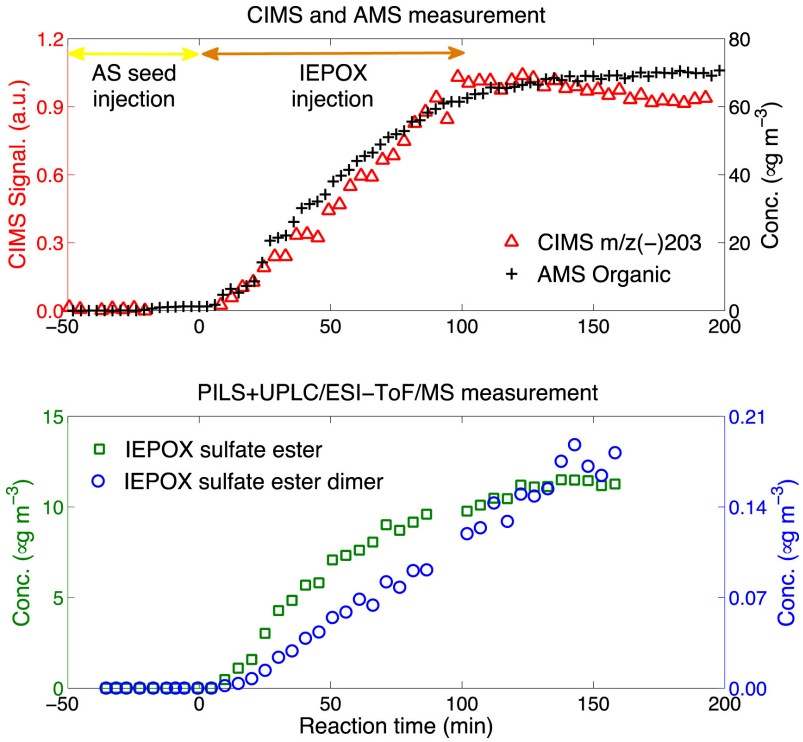

Figure F.6: Temporal profiles of normalized CIMS signals at *m/z* (-) 203, which represents the fluoride cluster product of IEPOX ($C_5H_{10}O3{\cdot}CF_3O^-$), and AMS measured total organic (upper panel), as well as IEPOX-derived sulfate ester and dimer measured by the PILS + UPLC/ESI-Q-TOFMS technique (lower panel).

remaining 100 min of the experiment, AMS measured total organic mass is at a steady state, whereas the CIMS signal at *m/z* (-) 203 exhibits a slow decay, which is likely a result of vapor wall losses of epoxide at high RH in the chamber.

For the PILS collected samples, the dominant ion observed in the UPLC/ESI-Q-TOFMS mass spectra in the negative mode is $C_5H_{11}SO_7^-$, which corresponds to the IEPOX-derived hydroxyl sulfate ester. The hydroxyl sulfate ester dimer $C_{10}H_{22}SO_{10}^-$ is also observed in the form of $[M\text{-}H]^-$. Corresponding normalized mass spectra and temporal profiles of these two products are shown in Figure F.7 and the lower panel of Figure F.6, respectively. Prompt formation of sulfate ester was observed at the onset of IEPOX injection, and the time-dependent trend agrees with the AMS measured organic aerosol growth curve. The sulfate ester dimer, on the other hand, exhibits a 20 min induction period and creeps up over the course of the experiment. As authentic standards for IEPOX-derived organosulfates are not commercially available, the UPLC/ESI-Q-TOFMS was externally calibrated with a surrogate quantification standard, d-galactone 6-sulfate sodium salt (Sigma Aldrich

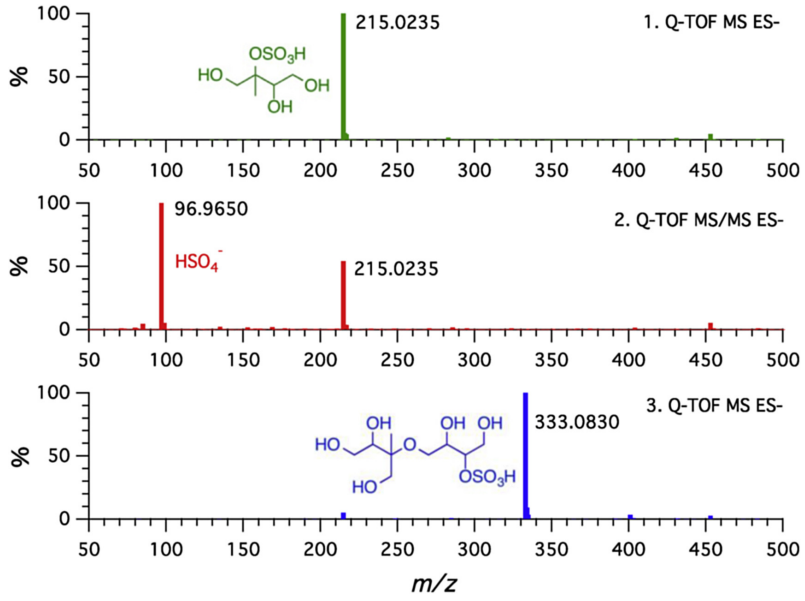

Figure F.7: (Panel 1) Mass spectrum for the IEPOX-derived hydroxyl sulfate ester, detected as *m/z* = 215 in the form of $C_5H_{11}SO_7^-$ ($[M\text{-}H]^-$). (Panel 2) The MS/MS fragmentation confirms the organosulfate with the *m/z* 97 (HSO_4^-) daughter ion. (Panel 3) Mass spectrum for the IEPOX-derived hydroxyl sulfate ester dimer, detected as *m/z* = 333 in the form of $C_{10}H_{20}SO_6^-$ ($[M\text{-}H]^-$).

> 98%), the elemental composition and functionality of which most closely resemble that of the IEPOX-derived organosulfates. An ESI/MS response factor of 1.56×10^{-5} ppm/area, is obtained for the d-galactone 6-sulfate anion ($C_6H_{11}SO_9^-$) at *m/z* 259 and applied to quantify the IEPOX-derived organosulfate ester and dimer. This sensitivity gives the overall equilibrium particle-phase organosulfate concentration of ~12 μg m^{-3}, which accounts for 17% of the AMS measured total organic masses. Note that although both belong to the organosulfate family and readily fragment to bisulfate anion (HSO_4^-) in the MS/MS analysis, the molecular properties of d-galactone 6-sulfate ($C_6H_{11}SO_9^-$) and IEPOX-derived sulfate ($C_5H_{11}SO_7^-$) that affect the ESI ionization efficiency, such as pK_a value, hydrophobicity, surface activity, *etc.*, are not exactly the same. One should expect that the ESI-MS responses for these two organosulfates differ even under identical instrument operation conditions, and as a result, the conclusion that IEPOX-derived organosulfates account for 17% of the AMS measured total organic masses has a degree of uncertainty.

F.5 Conclusions

We introduce here the combination of two well-established analytical techniques, PILS and UPLC/ESI-Q-TOFMS, for time-resolved and quantitative measurement of

chamber-generated organic aerosol chemical composition. The PILS + UPLC/ESI-Q-TOFMS system shows its promising utility, including relatively high-time resolution that allows for the investigation of aerosol dynamics and soft ionization to identify the integral molecular structure of particle-phase components. Additionally, the incorporation of liquid chromatography allows the pre-separation of species prior to the electrospray ionization, thus making the quantification of individual compounds plausible.

The PILS collection efficiency (CEPILS) towards a population of sub-micron particles composed of pure chemical standards, including carboxylic acids, polyols, and amines, is estimated by simultaneously comparing the DMA vs. UPLC/ESI-Q-TOFMS measured total organic mass concentrations. The overall mass collection efficiency exceeds 0.6 for particles with water solubility of >1 g L^{-1}, which corresponds to an average O:C ratio of >0.26. The AMS measured O:C ratios for SOA produced from photooxidation of a variety of VOCs (*e.g.*, isoprene, toluene, m-xylene, α-pinene, and naphthalene) in chamber experiments exceed 0.3, for which it is possible to characterize time-resolved chemical composition of these SOA systems at the molecular level. Instrument sensitivity and linearity were tested using single component organic aerosols generated from sorbitol, azelaic acid, pinonic acid, and adipic acid.

The PILS + UPLC/ESI-Q-TOFMS method is then applied to study the SOA formation driven by reactive IEPOX uptake onto hydrated and acidic ammonium sulfate particles. For the first time, time-resolved traces of IEPOX-derived organosulfate ester and dimer are observed. The temporal profile of the organosulfate ester is essentially identical to the AMS observed organic growth curve. The equilibrium organosulfate concentration potentially accounts for a significant fraction of the overall organic aerosol mass resulting from reactive IEPOX uptake. The combination of PILS collection with UPLC/ESI-Q-TOFMS analysis offers a new approach for time-resolved and quantitative characterization of aerosol constituents at molecular level.